UNIVERSITY
OF GÄVLE

FACULTY OF ENGINEERING AND SUSTAINABLE DEVELOPMENT

Behavioral Modeling of Power Amplifier with Memory Effect and Linearization Using Digital Pre Distortion

Om Prakash Nandi

September 2016

Master's Thesis in Electronics

Master's Program in Electronics/Telecommunications

Examiner: Magnus Isaksson

Supervisor: Raihan Rafique

Preface

This thesis work has been carried out in Ericsson, Lund; under Business Unit Radio Access Department and it is a part of the development of using high efficient and cost effective Power Amplifier in Small Cell Base Stations complying the regulations. I have been excited with this project exceptionally by the variety of scientific sectors it covered. I am very much pleased to get this valuable experience at Ericsson and for this I want to thank my supervisor, Raihan Rafique and manger Jacob Mannerstråle for giving me the opportunity to conduct my Master's thesis with Ericsson. Moreover, this work couldn't have been conducted without the effort of Raihan Rafique. I would like to express my gratitude to him for his tireless advice and scientific guidance, which helped me to complete this work. Surely, without his support, things would have been very difficult. However, I would like to thank all the people who have helped me in Ericsson throughout this journey. I am also grateful to my thesis partner Ibrahim Can Sezgin, for helping me throughout the whole project. Without his contribution, this project would have taken much more time. We conquered a lot of difficulties together. Moreover, I would like to thank him for being a good friend during my thesis work and my stay in Lund. I want to thank all the teachers of University of Gävle, for helping me to complete my Master's Degree. Next, I want to express my thanks to my family and my friends. These are the people who didn't involve physically in the project but supported me a lot during my work. I want to mention few names of my friends among a lot: Shampa Biswas, Raju Das, Motasim Ahmed for their support during my stay in Sweden. Further, I want to take the opportunity to show my appreciation to my parents, my sister and my affection to my two little nieces. Without their support, surely, it would not be possible for me to reach at this position in life. Finally, I want to gratefully acknowledge 'Swedish Institute' for believing in my potential and support me with the financial aid to complete my Master's studies in Sweden.

Abstract

This thesis work studied the behavioral modeling, estimation of parameters, model performance and linearization of power amplifier (PA) using Digital Pre Distortion (DPD) technique. PAs are one of the fundamental block in communication systems and also one of the main sources of nonlinearities in the system, as these devices are frequently subjected to signals characterized by considerable bandwidths and non-constant envelopes due to use of modern modulation technique. Moreover, PAs have high efficiency level at its nonlinear region. So, to operate the PA at its high efficiency region, linearization operation needs to be done. This has been investigated in this thesis work with the help of behavioral modeling and DPD. An essential initial step in designing a linearizer for a PA is to model the PA nonlinearity accurately. Behavioral modeling has been used for PA model for its computational efficiency, which means by relating input and output signals without addressing to the physical analysis of the device. DPD technique has been chosen for linearizing the performance of PA based on their low requirement of resources for implementation. In this thesis, five different PA models with memory effect, based on Volterra series, are studied and compared for three different PAs selected by Ericsson. These PAs are designed for third and fourth generation telecommunication system. Two different signals with different peak to average ratios and different bandwidths have been used as input signals of PA for this study. The main result in this thesis work includes the comparison of all five forward behavioral modeling results for all three PA's. The results also describe that; two of the given PA's can be linearized by using the DPD technique within the 3GPP standard regulations for ACPR.

Table of contents

List of figures

List of Tables

Notation

PA	Power Amplifier
DPD	Digital Pre Distortion
3GPP	3rd Generation Partnership Project
ACPR	Adjacent Channel Power Ratio
W-CDMA	Wideband Code Division Multiple Access
OFDM	Orthogonal Frequency Division Multiplexing
PAPR	Peak to Average Power Ratio
LTE	Long Term Evolution
CEPT	Conference of Postal and Telecommunications Administrations
MP	Memory Polynomial
GMP	Generalized Memory Polynomial
SV	Simplified Volterra
ACRGMP	Augmented Complexity Reduced Generalized Memory Polynomial
ACRSV	Augmented Complexity Reduced Simplified Volterra

1 Introduction

The radio frequency (RF) power amplifier (PA) is a decisive component in modern telecommunication system. It is a key element in transmitter as it is in charge of amplifying the RF input signal as a function of DC power and supply the RF output power to the transmitting antenna of the communication link with enough power to be detected by the receiver for a successful transmission. Further, PA is the most power demanding device of the transmission link and the more the signal is amplified, more power the PA consumes and with high power it inherently behaves nonlinearly i.e. PA cannot amplify the input as expected after its specific limiting range. However, with the increase in input power, the efficiency of PA also increases. Therefore, in RF PAs there is a trade-off between efficiency and linearity. High efficiency and high linearity cannot be achieved at the same time directly. Moreover, the modern technologies, which are widely used in wireless communication industry due to the requirement of high data rate, such as Wideband Code Division Multiple Access (W-CDMA) and Orthogonal Frequency Division Multiplexing (OFDM) use non-constant envelopes for data transmission [1]. Along with this inconsistent envelope, these technologies have high peak to average power ratio (PAPR). For the PA to be linear when transmitting the symbols with high peak power, the average PA output power needs to be several dB lower (approximately PAPR of input signal value) than the compression point, which decreases the overall efficiency [2]. Together with the nonlinear behavior of the PA, it enlarges the interference problem and leads to spreading of the transmitted spectrum, which is often referred to as spectral regrowth. One solution for this problem is to use a highly linear PA, but the design of linear and efficient PAs in modern radio telecommunication systems has been described in the literature as one of the most challenging design problems [3,4]. Another solution is to use a linearizer for the PA. One of most widely accepted technique is the Digital Pre Distortion (DPD) [3,4,5]. In order to work with DPD, it requires the knowledge of nonlinear characteristic of PA, since DPD implies the inverse of the PA model to the input signal before feeding into PA block. Accurate PA model is necessary in this context. Behavioral PA model is in immense interest that can characterize the PA without any prior knowledge of internal circuitry. In this thesis work, five different behavioral models of PA have been described and implemented. Later on, these models are used to generate the linearizer for PA and analysis its linearization performance with respect to 3GPP standard.

This thesis report has been divided into five main chapters including this chapter I. Further; Chapter II describes the theoretical background of PA characteristics, behavioral modeling and DPD technique. Chapter III consists of PA modeling and linearization implementation procedure, experimental setup and results. Chapter IV discusses the results followed by Chapter V, which concludes the report.

2 Theory

2.1 Introduction

This chapter is divided into seven different parts and discusses all theoretical study used on this thesis work. First part describes basics of Power Amplifier; characteristics are also explained as well. In the second part, nonlinear PA behavioral modeling is explained. Five different nonlinear PA model based on Volterra series are studied. Next section deals with the theory of identification procedure of described models, which is parameter extraction to create the model. Section five presents the comparison of all models in context of complexity. Benchmark for PA modeling and Digital Pre Distortion (DPD) performance discussed in next section. Last Section points out the procedure for linearizing PA and elaborates the theoretical concept of DPD.

2.2 Power Amplifier Overview

PA is one of the most fundamental components for wireless communication system. It converts DC power into RF output power, as a function of RF input power [6]. It is used to amplify the signal before transmitting by Antenna without creating too much noise so that it can be detected by the receiver and it should avoid amplifying the signals out of desired bandwidth. PA is the highest power consuming device in RF transmitting link; accordingly, power consumption of PA is another deciding consideration. In this section, different properties of PA will be presented along with their effect on the overall performance.

2.2.1 Gain and Gain Compression

The power gain of a power amplifier is defined by the ratio of output power to the input power. It is usually represented in decibel as [6]

$$G_{db} = 10\log_{10}\left(\frac{P_{out}}{P_{in}}\right) \tag{2-1}$$

Where, P_{out} is the power delivered to the load and P_{in} is the input power. Gain of PA depends on many factors related to the properties of the transistors used in the PA. It is an inherently nonlinear device; the PA gain is not constant, moreover, it depends on the individual device internal circuitry, RF input power, frequency and DC input power. However, over a certain bandwidth and input power range PA gain considered as constant. The PA output power is in increasing nature with the increase input power for a constant DC power. But, once it the output power reaches at a certain limit, the gain is not

constant anymore and the PA is in Gain compression / Saturation region. This is the instant when the PA starts to show its static distortion nonlinear characteristics. At this region, the output power doesn't increase with the increase of input power. The output power, where the actual gain is 1 dB below a linear gain is defined as the 1 dB compression point (P1 dB) refers to PA output. Below figure 2-1 shows the gain characteristic and 1 dB compression point of one of the PA we used in our thesis work with 27dB gain. The gain characteristic curve has been obtained from software simulation.

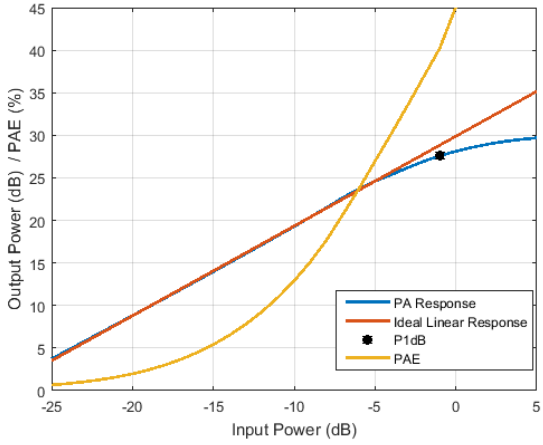

Figure 2-1: Input Output Characteristic with PAE of an Ideal PA and Real PA

2.2.2 Efficiency

In absolute world, all input power to a PA should be transformed into amplified RF output power. But, in real situation and some portion of the input power can be converted into output power. Power efficiency is the measure of indication of this power conversion. The efficiency can be described in two ways: drain efficiency and power added efficiency (PAE) [7,8]. Ratio of RF output power to the supplied DC Power to PA is defined as drain efficiency.

$$\mathrm{D} = \frac{P_{out}}{P_{DC}} \tag{2-2}$$

Where, P_{out} is the power delivered to the load from PA and P_{DC} is the supplied power. In drain efficiency RF input power is not considered. However, it is more common to define the efficiency of PA in PAE. This is calculated form the ratio of difference between RF output power and RF input power to supplied power. PAE reflects the efficiency of the DC power in terms of gain.

$$PAE = \frac{P_{out} - P_{in}}{P_{DC}} \tag{2-3}$$

Here, P_{in} is the RF input power to PA. With the increase of Output power PAE also increases. It can be seen from figure 2-1.

2.2.3 Nonlinearity of PA

From figure 2-1, it's been noted that, the maximum power efficiency generally occurs when the PA is running in its saturation region. On the other hand, all PA have nonlinear properties, which become prominent at their saturation region. It can be seen from below figure 2-2. For a sinusoidal input signal, if the PA follow it's the linear curve the output will also be similar as sinusoidal but with amplifying amplitude. But, as inherently PA behavior is nonlinear. At high input power, the PA characteristic follows the red curve and accordingly, the peaks get compressed for the output power.

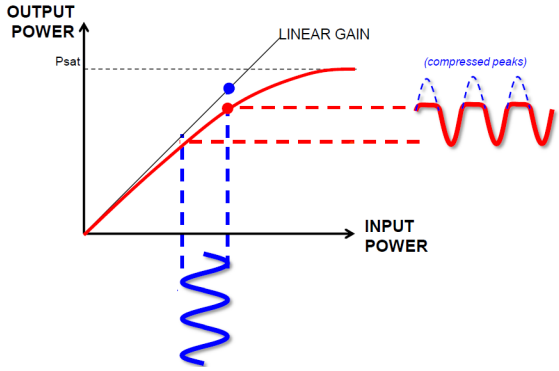

Figure 2-2: Nonlinear Operation of PA (Compressed Peaks)

These compressed peaks at time domain has a spectral growth effect in frequency domain. Figure 2-3 showing the effect of clipping of signals. This simulation is done in mathematical environment. It shows a sinusoidal wave of 1 MHz frequency and corresponding frequency domain response in figure 2-3 (a). And, figure 2-3(b) shows when the same signal is clipped 5%. As it can be seen, when there is clipping, frequency spectrum of the signal grows even for a single tone input signal. Accordingly, for multi tone signals such as long term evolution (LTE) signals, the intermodulation products caused the spectral growth in undesired band due to this PA nonlinear behavior.

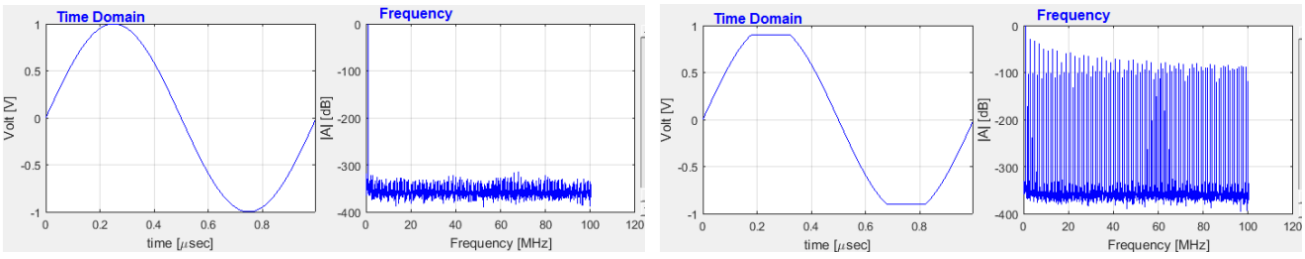

(a) *(b)*

Figure 2-3: 1 MHz Sinusoidal signal response (a) without clipping (b) with clipping

A sample is shown in figure 2-4 for 20 MHz LTE signal. For high input power level (-10 dBm) the PA response shows high spectral growth compare to lower input power level (-20 dBm). This is a

measurement result from one of the PA measurement in this thesis. These non-linear characteristics of a power amplifier make linearization procedures inevitable for high power efficiency modes.

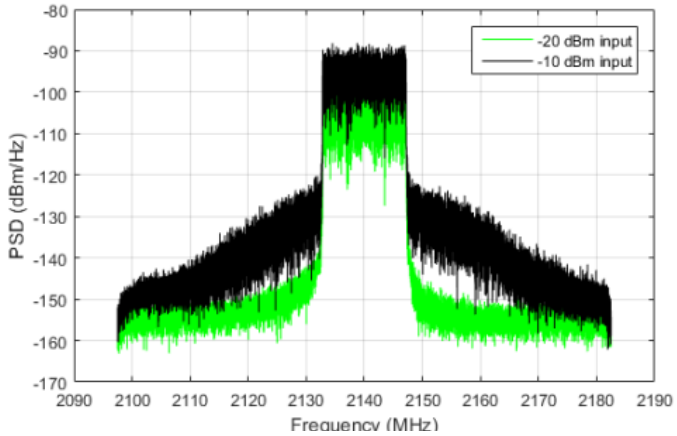

Figure 2-4: Two different output response with different input power levels.

Moreover, as discussed, there is a trade off on selecting the operating point of a PA. To have the maximum PAE and maximum output power PA operates in the nonlinear region [5]. In presence of wideband signals having non constant amplitude PA behave as nonlinear system and it exhibits two types of nonlinearities; static distortion and memory effects [9]. From the characteristic of a PA in figure 2-1 it is visible that, at certain condition, RF input power and RF output power relation is not linear, which explained in figure 2-2 and figure 2-3. This is static distortion. Further, due to transistor characteristic, PA shows the memory effect distortion.

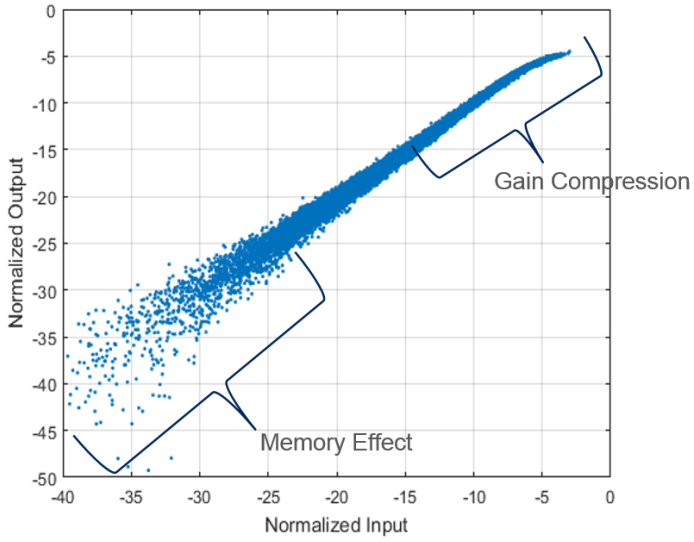

Figure 2-5: Memory Effect and Gain Compression of PA

The term memory used here describes the effects that vary on timescales much longer than those associated with the RF period that is; the output of the PA at time t_0 is not only depends on the input at t_0 but also depends on $t_0-1, t_0-2, \ldots, t_0-m$. Here m is the memory depth [4,10]. Two types of

memory effects, short term and long term memory can be categorized depending on the length of memory depth. Memory effects in PA caused by the dynamic self-heating and the trapping of charges in transistors. Figure 2-5 shows the PA characteristic showing the nonlinearities of a PA, which used in this thesis work. The PA was stimulated with a 20MHz LTE signal at its 1dB compression point. The nonlinearities of PA exhibit two different trends. At low input power level, a mild static nonlinearity with strong memory effects (Output values are spread over a range) and in contrast to that at high input power level static nonlinearity (Output values not following the linear slope) become dominant with mild memory effects [9].

2.2.4 AM/AM and AM/PM Characteristic

To characterize, the linearity of AM/AM and AM/PM curves of PA are analyzed [11]. Generally, RF PA operates in a certain limited band and they are baseband in nature. Accordingly, mathematical representation also shortened within that region. So, to use complex envelop notation is much more convenient while describing a PA. If the input signal to a PA be,

$$x(t) = a(t)e^{j\varphi(t)} \tag{2-4}$$

Where, $a(t)$ is the envelop and the $\varphi(t)$ is phase of the input signal and $j = \sqrt{-1}$. The output response of the nonlinear PA, $y(t)$ will be the amplified distorted version of the $x(t)$. The output can be represented as,

$$y(t) = g[a(t)]\exp[j\varphi(t) + f(a(t))] \tag{2-5}$$

Whereas function g and f appears due to the non-ideal behavior of the PA and denoted as Amplitude to Amplitude (AM/AM) and Amplitude to Phase (AM/PM) distortion. Figure 2-6 shows the AM/AM and AM/PM distortion of PA used in this Thesis with 27dB gain. The measurements were done with a 20MHz wide LTE signal at 2.14GHz center frequency.

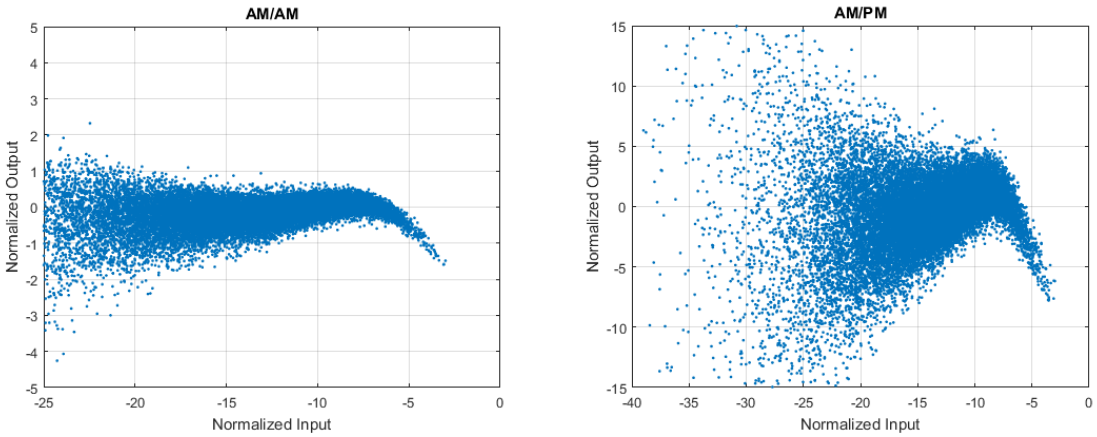

Figure 2-6: Measured AM/AM and AM/PM Distortion

2.3 Power Amplifier Modeling

Modeling of any RF device or system can be classified into two main groups [12,13], namely physical/circuitry models and Empirical models. Physical models are based on fundamental physics of device. Additionally, electrical circuit elements and circuit theory are used to model the system [14]. On the other hand, empirical models are based on the sampled measured input and output data. To model the system, little or no knowledge of the internal circuit is required. That's why this type of modeling is also called Black-box modeling or Behavioral modeling. Technology independence and protection of intellectual property is the main advantage of using Behavioral model, as it doesn't deal with the internal circuitry information [15]. Depending on the distortion this Behavioral model can be classified into memoryless models (output envelop reacting instantaneously to variations of the input envelop), linear memory models (BMs that account for envelope memory effects attributable to the input and output matching networks' frequency characteristics) and nonlinear memory models (dynamic interaction of nonlinearities through a dynamic network) [12]. Static nonlinear models with memory (based on Volterra Series) are examined in this thesis as, nonlinear memory models, which can represent the PA considering its high nonlinear effects with memory as discussed in section 2.2.3. Neural Network (NN) modeling can also model the nonlinear memory effect of PA [16], which is not part of this thesis investigation.

2.4 Volterra Series Based Model

The Volterra series is a universal mathematical tool to describe any nonlinear function with memory effects. In late 19th century Vito Volterra described this Volterra series and the theory behind this. The continuous time Volterra series can be represented by following [17],

$$y(t) = h_0 + \sum_{n=1}^{N} \int_a^b \ldots\ldots \int_a^b h_n(\tau_{1,\ldots\ldots,}\tau_{n,}) \prod_{j=1}^{n} x(t-\tau_j) d\tau_j$$

(2-6)

Where x and y represents the input and output respectively, h_0 is a constant term and $h_n(\tau_{1,\ldots\ldots,}\tau_{n,})$ are the n^{th} order coefficients of the Volterra series often called Volterra kernels of the system. Power amplifiers can be considered as a causal system as the PA's output depends on the instantaneous input and the previous input. In the absence of input, h_0 in the formula becomes zero as the output is zero for a causal system. This Volterra series can be described as a generalized Taylor series with memory [18]. In discrete time domain baseband representation of the Volterra series can be formulated by following [16,17],

$$y(n) = \sum_{\substack{p=1 \\ p-odd}}^{P} \sum_{m1=0}^{M} \sum_{m2=m1}^{M} \ldots\ldots\ldots \sum_{m(p+1)/2=m(p-1)/2}^{M} \ldots\ldots \sum_{(p+3)/2=0}^{M} \ldots \sum_{mp=mp-1}^{M} h_p(m_1, m_2, \ldots m_p) \prod_{i=1}^{(p+1)/2} u(n-m_i) \prod_{(p+3)/2}^{p} u*(n-m_j)$$

(2-7)

Where, first summation is restricted to odd values of P. $h_p(m_1, m_2, \ldots m_p)$ are the kernels for the Volterra model and $(.)*$ represent the complex conjugate. P is the nonlinear order and M is the memory depth. The Volterra series model can provide good accuracy for PA modeling theoretically, but unfortunately the number of parameters increases drastically with the increase of nonlinear order and memory length, causes high computational complexity. Moreover, with increased number of parameters reduced the Volterra series usefulness for only mildly nonlinear systems [12], and to curtail the parameter numbers and for simplification several models are proposed. This Thesis investigate the five different Volterra Based models for PA modeling namely, Memory Polynomial (MP) [19], Generalized MP (GMP) [20], Augmented Complexity Reduced GMP (ACRGMP) [21], Simplified Volterra (SV) [22], Augmented Complexity Reduced SV (ACRSV) [23].

2.4.1 Memory Polynomial Model

Memory Polynomial (MP) model is widely known behavioral model based on reduction of Volterra Series model. Reduction of Volterra series has been implemented to reduce the complexity within the limited resource. This model only takes the diagonal terms of the Volterra series and its mathematical formulation given [19],

$$y_{mp}(n) = \sum_{m=0}^{M} \sum_{k=1}^{K} a_{mk} x(n-m) \left| x(n-m) \right|^{k-1}$$

(2-8)

Where, $x(n)$ and $y_{mp}(n)$ are the input and output of the MP model respectively. K, M and a_{pm} represents the maximum nonlinearity order, memory depth and the kernels of the MP model respectively. ($|\,|$) denotes the absolute value. Equation 2-8 model the output from input signal and it's corresponding envelop for the same memory instance. Altering the value of K and M in the equations, PA model can be controlled for high accuracy and number parameters.

2.4.2 Generalized Memory Polynomial Model

Another model based on Volterra series is Generalized Memory Polynomial Model (GMP). This model is an extension of MP model by introducing products between the input signal and envelop terms with different time shift (leading/lagging). These additional terms in GMP model compare to MP models are specified as cross terms. Mathematical formulation of GMP model combined three branches as follows [20,21],

$$y_{GMP}(n) = \sum_{m=0}^{M_a-1}\sum_{k=1}^{K_a} a_{mk}x(n-m)\left|x(n-m)\right|^{k-1} + \sum_{m=0}^{M_b-1}\sum_{l=1}^{L_b}\sum_{k=2}^{K_b} b_{mlk}x(n-m)\left|x(n-m-l)\right|^{k-1} + \sum_{m=0}^{M_c-1}\sum_{l=1}^{L_c}\sum_{k=2}^{K_c} c_{mlk}x(n-m)\left|x(n-m+l)\right|^{k-1} \tag{2-9}$$

Where, $x(n)$ and $y_{GMP}(n)$ are the input and output signals for the GMP model. M_a, K_a and a_{mk} are the memory depth, nonlinearity order and model parameters or kernels of aligned terms between input signal and it's envelop respectively. This branch of equation is same as the MP model. Next two branch will add the cross terms. M_b, K_b L_b and b_{mlk} are the memory depth, nonlinearity order, lagging cross term index and model kernels of input signal and it's lagging envelop terms respectively. Similarly, M_c, K_c, L_c and c_{mlk} are the memory depth, nonlinearity order, lagging cross term index and model kernels of input signal and it's leading envelop terms respectively. By changing the M_b and M_c memory of the cross terms can be adjusted in the modeling formula. By adding lagging and leading cross terms PA modeling performance can be improved as shown in [20].

2.4.3 Simplified Volterra Model

Based on Volterra series and to increase the accuracy of the GMP model, Simplified Volterra (SV) model has been introduced in [22]. SV model is an extension of GMP model. It combines the GMP model with cross terms between the conjugate signal and lagging/leading envelop terms. The mathematical formula for SV model is shown in equation 2-10,

$$y_{SV}(n) = \sum_{m=0}^{M_a-1}\sum_{k=1}^{K_a} a_{mk}x(n-m)\left|x(n-m)\right|^{k-1} + \sum_{m=0}^{M_b-1}\sum_{l=1}^{L_b}\sum_{k=2}^{K_b} b_{mlk}x(n-m)\left|x(n-m-l)\right|^{k-1}$$
$$+\sum_{m=0}^{M_c-1}\sum_{l=1}^{L_c}\sum_{k=2}^{K_c} c_{mlk}x(n-m)\left|x(n-m+l)\right|^{k-1} + \sum_{m=0}^{M_d-1}\sum_{l=1}^{L_d}\sum_{k=2}^{K_d} d_{mlk}x*(n-m)x^2(n-m-l)\left|x(n-m-l)\right|^{k-1}$$
$$+\sum_{m=0}^{M_e-1}\sum_{l=1}^{L_e}\sum_{k=2}^{K_e} e_{mlk}x*(n-m)x^2(n-m+l)\left|x(n-m+l)\right|^{k-1}$$

(2-10)

Where, $x(n)$ and $y_{SV}(n)$ are the input and model output signals for the SV model. M_a, K_a and a_{mk} are the memory depth, nonlinearity order and model parameters or kernels of aligned terms between input signal and it's envelop respectively. M_b, K_b, L_b and b_{mlk} are the memory depth, nonlinearity order, lagging cross term index and model kernels of input signal and it's lagging envelop terms respectively. M_c, K_c, L_c and c_{mlk} are the memory depth, nonlinearity order, lagging cross term index and model kernels of input signal and it's leading envelop terms respectively. M_d, K_d, L_d and d_{mlk} are the memory depth, nonlinearity order, lagging cross term index and model kernels of conjugate of input signal and it's lagging envelope terms respectively. M_e, K_e, L_e and e_{mlk} are the memory depth, nonlinearity order, leading cross term index and model kernels of conjugate of input signal and it's leading envelope terms respectively.

2.4.4 Augmented Complexity Reduced GMP Model

As discussed in previous section 2.4.1, MP model considers the memory depth and nonlinearity order together, that ask for same nonlinearity order will be used for all branches. It results involvement of high complexity parameter calculation, which increases the computational cost. This phenomenon is more massive in GMP model (Section 2.4.2) as it also adds extra lagging and leading branches. Especially for a highly nonlinear PA, high values for nonlinearity order and memory depth has to be chosen, which increase the modeling complexity enormously. Therefore, to reduce the number of coefficient an efficient way is to split the nonlinearity and memory effect in the GMP Model as shown and an Augmented Complexity Reduced GMP (ACRGMP) model has been introduced in [21]. In this method, first of all the complexity reduced by splitting the nonlinearity and memory effect in GMP model, and later on added a parallel nonlinear memory effect (NME) block to improve the model performance. The NME block has been constructed using a third order Volterra filter. The mathematical formulation for ACRGMP model is as following [21],

$$u(n) = \sum_{k=1}^{K_a} r_k{}^{(a)}x(n)\left|x(n)\right|^{k-1}$$

(2-11)

$$y_{NME}(n) = \sum_{m=0}^{M_d-1} d_m \left|u(n-m)\right|^2 u(n-m)$$

(2-12)

$$y_{ACRGMP}(n) = \sum_{k=1}^{K_a} r_k^{(a)} \sum_{m=0}^{M_a-1} a_m x(n-m)\left|x(n-m)\right|^{k-1} + \sum_{k=1}^{K_b} r_k^{(b)} \sum_{m=0}^{M_b-1} \sum_{l=1}^{L_b} b_{ml} x(n-m)\left|x(n-m-l)\right|^{k-1}$$
$$+ \sum_{k=1}^{K_c} r_k^{(c)} \sum_{m=0}^{M_c-1} \sum_{l=1}^{L_c} c_{ml} x(n-m)\left|x(n-m+l)\right|^{k-1} + \sum_{m=0}^{M_d-1} d_m \left|u(n-m)\right|^2 u(n-m)$$

(2-13)

Where, in equation 2-11 $u(n)$ denotes the output a memoryless model for input $x(n)$ with nonlinearity order K_a and $r_k^{(a)}$ defines the kernels for this memoryless model. Further, $y_{NME}(n)$ is the output of NME block presented in equation 2-12 where, d_m presents the coefficients of the Volterra filter and M_d is the memory depth of the filter. Combining equation 2-11 and 2-12 and model equation 2-9 for GMP model, gives the ultimate output equation of the ACRGMP model describes in equation 2-13. In this equation, $x(n)$ and $y_{ACRGMP}(n)$ are the input and output signals for the ACRGMP model. M_a, K_a, $r_k^{(a)}$ and a_m are the memory depth, nonlinearity order, memoryless nonlinear model kernel and memory nonlinear model kernels of aligned terms between input signal and it's envelop respectively. M_b, K_b, L_b, $r_k^{(b)}$ and b_{ml} are the memory depth, nonlinearity order, lagging cross term index, memoryless nonlinear model kernels and memory nonlinear model kernels of input signal and it's lagging envelop terms respectively. M_c, K_c, L_c, $r_k^{(c)}$ and c_{ml} are the memory depth, nonlinearity order, leading cross term index, memoryless nonlinear model kernels and memory nonlinear model kernels of input signal and it's leading envelop terms respectively [21].

2.4.5 Augmented Complexity Reduced SV Model

Section 2.4.3 describes the SV model, which adds more terms to the GMP modeling of PA. This increase the complexity of the model as number of model kernels increases more in SV model compare to GMP model. As discussed for ACRGMP in section 2.4.4, same technique of splitting the nonlinear and memory effect can be implemented in SV model. This type of model named as Augmented Complexity Reduced SV (ACRSV) and introduced in [23]. This model is same as ACRGMP model and also adds a NME block to improve the model performance. The mathematical formulation can be deduce as,

$$y_{ACRSV}(n) = \sum_{k=1}^{K_a} r_k^{(a)} \sum_{m=0}^{M_a-1} a_m x(n-m)\left|x(n-m)\right|^{k-1} + \sum_{k=1}^{K_b} r_k^{(b)} \sum_{m=0}^{M_b-1}\sum_{l=1}^{L_b} b_{ml} x(n-m)\left|x(n-m-l)\right|^{k-1}$$

$$+\sum_{k=1}^{K_c} r_k^{(c)} \sum_{m=0}^{M_c-1}\sum_{l=1}^{L_c} c_{ml} x(n-m)\left|x(n-m+l)\right|^{k-1} + \sum_{k=1}^{K_d} r_k^{(d)} \sum_{m=0}^{M_d-1}\sum_{l=1}^{L_d} d_{ml} x*(n-m)x^2(n-m-l)\left|x(n-m-l)\right|^{k-1}$$
$$+\sum_{k=1}^{K_e} r_k^{(d)} \sum_{m=0}^{M_e-1}\sum_{l=1}^{L_e} e_{ml} x*(n-m)x^2(n-m+l)\left|x(n-m+l)\right|^{k-1} + \sum_{m=0}^{M_f-1} d_m\left|u(n-m)\right|^2 u(n-m)$$

(2-14)

Where, $x(n)$ and $y_{ACRSV}(n)$ are the input and model output signals for the ACRSV model respectively. M_a, K_a, $r_k^{(a)}$ and a_m are the memory depth, nonlinearity order, memoryless nonlinear model kernels and memory nonlinear model kernels of aligned terms between input signal and it's envelop respectively. M_b, K_b, L_b, $r_k^{(b)}$ and b_{ml} are the memory depth, nonlinearity order, lagging cross term index, memoryless nonlinear model kernels and memory nonlinear model kernels of input signal and it's lagging envelop terms respectively. M_c, K_c, L_c, $r_k^{(c)}$ and c_{ml} are the memory depth, nonlinearity order, leading cross term index, memoryless nonlinear model kernels and memory nonlinear model kernels of input signal and it's leading envelop terms respectively. M_d, K_d, L_d, $r_k^{(d)}$ and d_{ml} are the memory depth, nonlinearity order, lagging cross term index, memoryless nonlinear model kernels and memory nonlinear model kernels of conjugate input signal and it's lagging envelop terms respectively. M_e, K_e, L_e, $r_k^{(e)}$ and e_{ml} are the memory depth, nonlinearity order, leading cross term index, memoryless nonlinear model kernels and memory nonlinear model kernels of conjugate input signal and it's leading envelop terms respectively. d_m represents the coefficients of the Volterra filter and M_f is the memory depth of the filter.

2.5 Model Parameter Identification

In previous sections, five different behavioral PA modeling has been introduced. These models are mathematical equations with unknown coefficients which also known as kernels. These coefficients can be extracted from input signal and output signal data of PA by model parameter estimation. For a chosen model, the model parameters or kernels have to identify to fit the experimental data of the PA. Least square estimate algorithm is a widely used method to estimate the model parameters. MP, GMP and SV model parameters can be identified by this least square method, as these models are linear in parameters. The least square algorithm assured global convergence [24]. But a single step least square method cannot solve for ACRGMP and ACRSV model as they combine multiple boxes (Nonlinearity without memory and NME) as discussed in section 2.4.4 and 2.4.5 respectively. So, for best estimation of parameters in these two models iterative process has been implemented. However, the iteration process for ACRGMP and ACRSV usually converges very fast [22,23].

2.5.1 Least Square Estimation Algorithm

Least square estimation algorithm [25] is introduced by A. Legendre. Basic idea for this estimation is to minimize the sum of the square residuals (ε) which is the difference between the measured data $y(n)$ and the data $\hat{y}(n)$ obtained from the Model [16],

$$\varepsilon = \sum_{n} \left| \hat{y}(n) - y(n) \right|^2$$

(2-15)

Here, n is the number of samples of the input $x(n)$ and output $y(n)$ signals. As described in earlier sections, mathematical equation for MP, GMP and SV model can be written more compactly in a vector equation,

$$\mathbf{y}_{n\times 1} = \mathbf{X}_{n\times k}\boldsymbol{\beta}_{k\times 1}$$

(2-16)

Where, $\mathbf{y}$ is vector of output data, $\mathbf{X}$ is matrix of state values derived from input data, $\boldsymbol{\beta}$ is the vector for unknown parameters. The least square solution for this will be,

$$\boldsymbol{\beta} = (\mathbf{X}'\mathbf{X})^{-1}\mathbf{X}'\mathbf{y}$$

(2-17)

Considering that, the inverse matrix of $\mathbf{X}'\mathbf{X}$ exists, that is the number of parameters to be estimated will be smaller than the number of measurement points and the parameters are linear in nature.

2.5.2 Iterative Process

Since models like ACRGMP and ACRGSV, based on nonlinear parameters, iterative process is implemented for parameter estimations. It should estimate coefficients of the model by least square algorithm separating memoryless nonlinearity and the memory nonlinearity on step-and-repeat operation. Parameter estimation for ACRGMP model is presented here. Firstly, two coefficient vectors $\mathbf{R}$ and $\mathbf{T}$ need to form. $\mathbf{R}$ consist of the memoryless nonlinearity coefficients and $\mathbf{T}$ consist of conventional memory effect coefficient, leading / lagging effect and third order Volterra filter.

$$\mathbf{R} = [r_1^{(a)}, \ldots, r_{Ka}^{(a)}, r_1^{(b)}, \ldots, r_{Kb}^{(b)}, r_1^{(c)}, \ldots, r_{Kc}^{(c)}]^T$$

(2-18)

$$\mathbf{T} = [a_0, \ldots, a_{Ma-1}, b_{01}, \ldots, b_{0Lb}, \ldots, b_{Mb-1,1}, \ldots, b_{Mb-1,Lb}, c_{01}, \ldots, c_{0Lc}, \ldots, c_{Mc-1,1}, \ldots, c_{Mc-1,Lc}, d_0, \ldots, d_{Md-1}]^T$$

(2-19)

At the starting point, two coefficient vectors are initializing as following,

$$\mathbf{R} = [1, 0, ..., 0]^T \tag{2-20}$$

$$\mathbf{T} = [1, ..., 0, 1, ..., 0, ..., 0, ..., 0, 1, ..., 0, ..., 0, ..., 0, 0, ..., 0]^T \tag{2-21}$$

As the iteration continues, the Least square method will give best result for $\mathbf{R}$ and $\mathbf{T}$. In each iteration, parameter estimation process consists of two steps. First step it to de-embed the output of the NME block from the output signal $y(n)$. Then equation 2-13 will be transformed into a linear parameter estimation problem coupled with $\mathbf{R}$ and can easily be solved and extracted with LS estimation method. The extracted parameters applied to input signal $x(n)$ and again $\mathbf{T}$ is extracted by LS method estimation method as well. Then the algorithm goes to next iteration process. The iteration can go on till a finite iteration number reached [21]. In this thesis while estimating with the ACRGMP model, this finite number fixed to 5. Similar approach has been taken for the parameter estimation of ACRSV model. Only difference is that it will have two additional terms for coefficients as discussed in section 2.4.5.

2.6 Model Complexity Comparison

Modeling of PA can be can be compared with each other in terms of performance or in terms of complexity (resource usage to calculate the number of coefficients). In this thesis work, the result section, all described five models will be examined according to their performance for a corresponding number of coefficients. The complexity of any model can be controlled by controlling the number of coefficients by restricting lower value of parameters. Depending on the application and precision required it can be fixed. Further the results in this thesis work also showed that with the increasing the number of coefficients i.e. non-linearity order, memory depth, cross terms memory depths will not necessarily increase the performance. There are some methods to estimate the optimum memory depth and non-linearity order for a specific PA is explain in [26,27,28]. In this thesis work, estimation of optimum parameters has not been investigated. Further, table 2-1 shows the mathematical expression for calculating the number of coefficients depending for corresponding parameters. Here, all the terms corresponding to the model equations explained in section 2.4.

Model	Total Coefficient Number
MP	$K(M+1)$
GMP	$K_a(M_a+1)+K_b(M_b+1)L_b+K_c(M_c+1)L_c$
SV	$K_a(M_a+1)+K_b(M_b+1)L_b+K_c(M_c+1)L_c+K_d(M_d+1)L_d+K_e(M_e+1)L_e$
ACRGMP	$K_a+K_b+K_c+(M_a+1)+(M_b+1)L_b+(M_c+1)L_c+(M_d+1)$
ACRSV	$K_a+K_b+K_c+K_d+K_e+(M_a+1)+(M_b+1)L_b+(M_c+1)L_c+(M_d+1)L_d+(M_e+1)L_e+M_f$

Table 2-1: Number of coefficient for different models

2.7 Linearization of PA by Digital Pre Distortion

As discussed in previous sections, RF PA's are the main cause for nonlinear behavior in modern telecommunication system. Therefore, several techniques are implemented to linearize PA, such as Power Back-off, Analog Pre Distortion and Digital Pre Distortion (DPD). As the PA is linear at the lower input power range, while the linearity becomes worse with the higher input power, one method to improve the linearity is to back-off the input power to linear region. This is called the power back-off technique [3]. But when back-off in the input power to linear region, the efficiency of the PA is reduced. It can be seen from figure 2-1. Basically, Power Back-off improves the linearity of the PA by sacrificing the efficiency, as the efficiency of PA is at best on its saturation. To obtain, both the linearity and high efficiency linearization techniques are required. Feedback and Feedforward are two types of Analog Pre Distortion techniques which can be found in [29] and [30] respectively. In this thesis, we used Digital Pre Distortion technique to linearize the PA performance.

2.7.1 DPD Architecture

The method for DPD will be discussed in this section. The basic idea of DPD is to identify the inverse function, H of the PA response and then used this function for predistorting the input signal $x(t)$ before it is fed to PA in such a way that the output signal $y(t)$ of the PA will be linearized as required signal $y_d(t)$. It can be mathematically formulated as following [3,16],

$$x(t) = H^{-1}[y_d(t)] \tag{2-22}$$

$$y(t) = H[x(t)] = H\{H^{-1}[y_d(t)]\} \tag{2-23}$$

If the inverse function H^{-1} is close to the inverse function to the real function H of the PA, the output $y(t)$ of the PA will be close to the required output $y_d(t)$. But, however, in practice all nonlinear systems are not invertible. But, but from [31,32] it is shown that, the inverse of Volterra system is itself a Volterra system. In [33] it has shown that, P[th] order pre inverse of a system is identical to its P[th] order post inverse. That is, it is possible to utilize the post inverse of a Volterra system and copy it as a pre inverse. Two types of method can implement to calculate the inverse function.

2.7.1.1 Direct Learning Architecture

This direct learning architecture is implemented by first creating a behavioral model of PA and later inverse the model. A block diagram of direct learning architecture is shown in figure 2-7. The model of PA has been created from the input $x(n)$ and PA response $y(n)$. From this model the inverse of the power amplifier behavioral model is used directly to construct the DPD. This architecture commonly utilizes iterative optimization procedures for the parameter of the DPD to minimize the error.

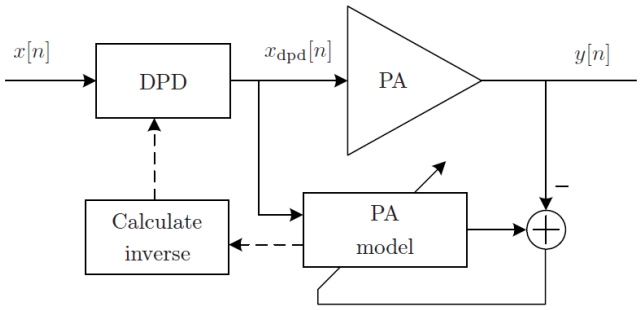

Figure 2-7: Direct Learning Architecture

2.7.1.2 Indirect Learning Architecture

The block diagram for an Indirect Learning Architecture is shown in figure 2-8. In this method, the output signal $y(n)$ is used as the input and the input signal $x(n)$ (which is the original signal before predistortion) is used as the output in the model algorithm to create the model of the PA. This is called the inverse model of PA. The inverse model block i.e. the post distorter block is copied before the PA as pre distorter block. Therefore, the input signal is first pre distorted by the inverse model then feed into the PA to get the desired output response. By iteratively estimating the inverse of the PA, final version of the Pre distorter can be found. This pre distorter can be used for digital predistortion for any signal with the same bandwidth for the given PA, i.e. if for a specific PA, post distorter block is calculated with certain number of iterations for a signal with a certain bandwidth, therefore, any signal that has the same bandwidth can be digitally pre distorted by using the same post distorter block without any iterations [34,35].

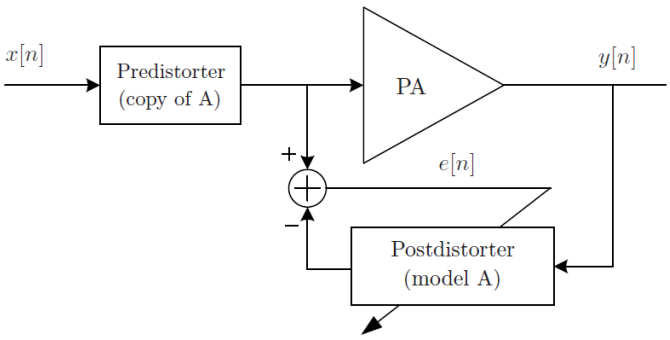

Figure 2-8: Indirect Learning Structure

2.8 Benchmark for PA Modeling and DPD Performance

In this thesis, two figure of merit has been taken into account to benchmark the performance of PA models and DPD performance. One of them is Normalized Mean Square Error (NMSE) which is used for PA modeling. The mathematical equation for NMSE is as follows,

$$NMSE_{db} = 10\log_{10}\left[\frac{\sum_{n=1}^{N}\left|y_{meas}(n) - y_{model}(n)\right|^2}{\sum_{n=1}^{N}\left|y_{meas}(n)\right|^2}\right] \tag{2-24}$$

Here, $y_{meas}(n)$ is the measured output response of PA, $y_{model}(n)$ is the modeled output which was created by estimating the coefficients from the measured data. The NMSE value defines how well the PA model can mimic the actual PA behavior. The block diagram in figure 2-9 shows this briefly.

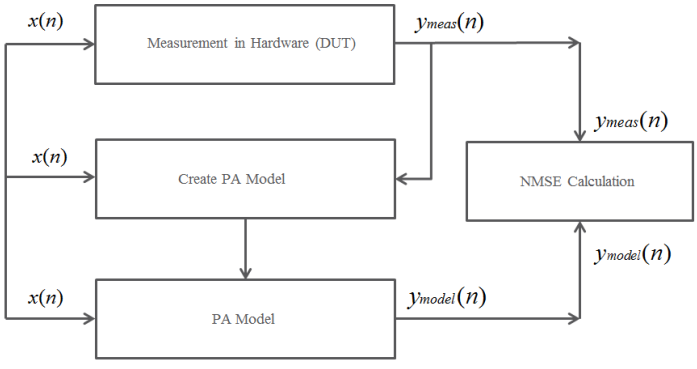

Figure 2-9: NMSE Calculation

Further, Adjacent Channel Power Ratio (ACPR) is considered for linearization performance of PA using DPD. ACPR is the ratio between the spectral power contained in the adjacent channel signal bandwidth and the spectral power contained in the main channel signal bandwidth. European Conference of Postal and Telecommunications Administrations (CEPT) is the controlling body for frequency spectrum in Europe. The details about the allocations can be found in [36]. These allocations cannot be violated for any wireless communication technique for any carrier frequency. 3GPP standards, define the maximum acceptable Adjacent Channel Power Ratio (ACPR) for the mobile phone communications for data transmission for 3G, LTE (4G). However, in this report the ACPR level that is checked is called ACPR1 and it can be seen on figure 2-10. Here it is shown for two 5MHz signal cascaded together with spacing of 15MHz at center frequency 2140MHz.

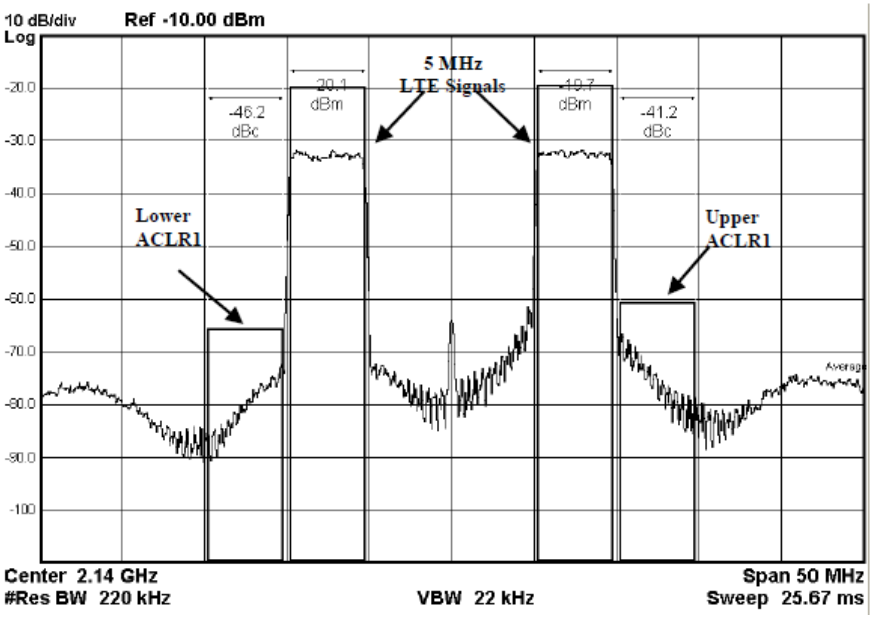

Figure 2-10: Adjacent Channel Power Ratio

3 Process and Results

3.1 Introduction

This chapter is divided into two main sections. One of them is process which describes implementation of the work procedures for generating the PA model and linearization of the same from the measurement setup and the next section shows the results obtain in the thesis work.

3.2 Process

3.2.1 Measurement Setup and Test Signals

In this thesis work, the identified models, which were discussed in previous chapter, have been extracted from the measurement data of PA. The measurement setup consisted with a vector signal generator (VSG) and vector signal analyzer (VSA) as shown in figure 3-1.

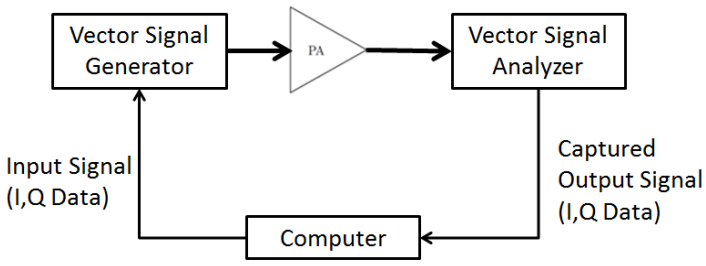

Figure 3-1: Outline of Measurement Setup

Here, in the backhand of the measurement setup, we used MATLAB environment in the computer to generate and capture the input and output complex envelop signal respectively. VSG and VSA are connected to the computer over local area network (LAN) connection for remote controlling and data handling. The VSG is capable of producing virtually any signal from complex-envelope data. We used MXG N5182B as VSG from Keysight, which has the capacity of clock frequency of 200 MHz and it can direct up conversion from baseband to RF. And the VSA was an MXA N9020A from Keysight, which samples the signal at low intermediate frequency using an analog-to-digital convertor at a maximum sampling rate of 106.25 MHz and gives analysis bandwidth of 85 MHz. To match with this capturing sampling rate, the input signals also created with a sampling rate of 106.25 MHz beforehand and the sampling clock of VSG also set to the same. Two different signals have been used as input signal for the modeling purpose with a carrier frequency of 2140 MHz. Test Signal-1 has a bandwidth of 25 MHz which consists of two cascaded 5 MHz LTE signal with a carrier spacing of 15 MHz and Test Signal-2 has a bandwidth of 40MHz, which consists of two cascaded 20MHz LTE signal. Both

the signals have 256 Quadrature Amplitude Modulation (QAM) scheme. Peak to average ratio for the Signal-1 and Signal-2 is 6.63 dB and 7.4 dB respectively. For linearization purpose only Signal-1 has been used.

3.2.2 Modeling and DPD Algorithm Implementation

The flow chart for implementing the Modeling algorithm of PA and linearization of the same using Digital Pre Distortion has been shown in figure 3-2(a) and 3-2(b).

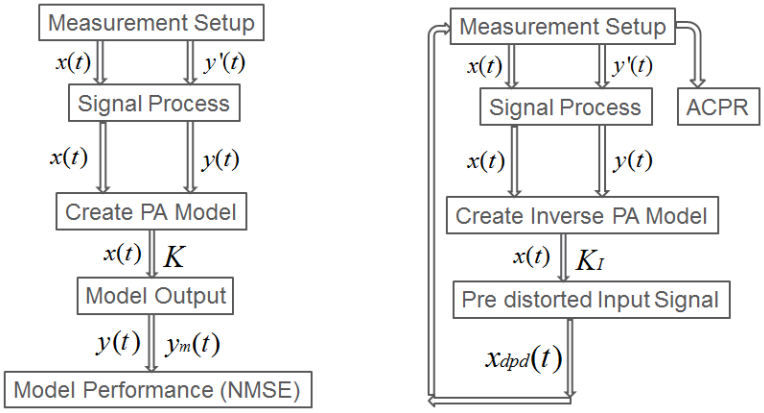

(a) PA Model *(b) DPD*

Figure 3-2: Implementation algorithms

From the measurement setup, after capturing the output response $y'(t)$ of a PA for a specific input signal $x(t)$, the output signal needs to be aligned with the input signal. Alignment is done by considering the cross correlation between the captured output and input signal. In the measurement setup shown in figure 3-2, the VSG is sending the input signal to DUT continuously. At certain time instant the output signal of DUT has been captured $y'(t)$. Then after calculating max cross correlation between the signals the captured output signal is shifted and aligned with the input signal.

Figure 3-3 shows the block diagram representation of the alignment and figure 3-4 shows the plotting of captured output $y'(t)$ and aligned output $y(t)$ envelop for 1st 200 samples.

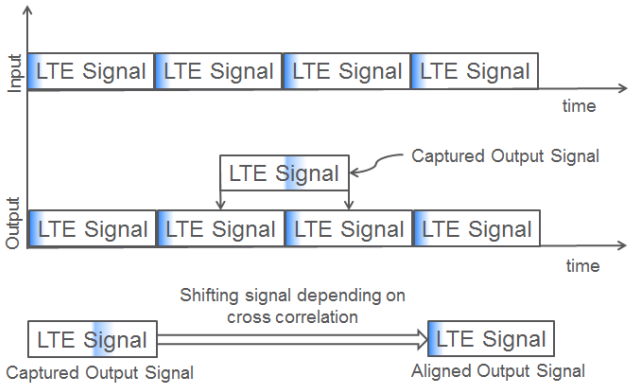

Figure 3-3: Alignment of captured output signal

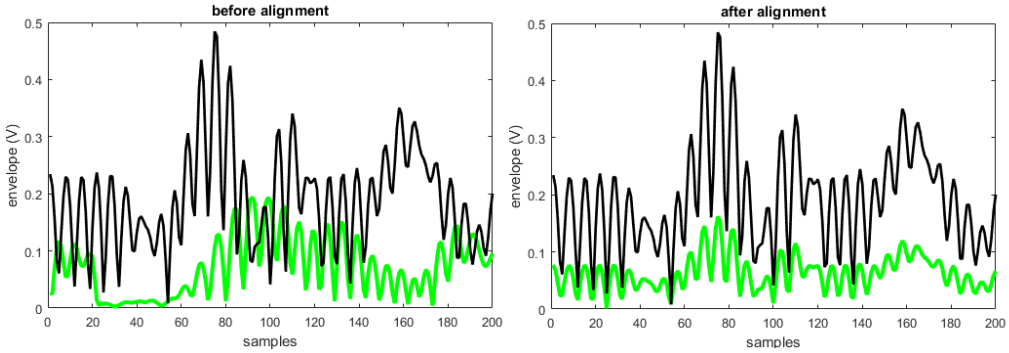

Figure 3-4: Envelop of captured output and aligned output with input signal.

After the alignment, input $x(t)$ and aligned output signal $y(t)$ are used to generate five different PA models i.e. calculation of model kernel K, figure 3-2(a). Model generation and estimation of kernels were described in details in chapter 2. After generating the PA model, the input signal $x(t)$ and K used to create the model output $y_m(t)$ and compare with measured aligned output $y(t)$, which gives the NMSE.

Accordingly, in DPD, apart from alignment of the captured output with input signal, gain normalization of the output signal should be done, so that the DPD algorithm can model the AM/AM and AM/PM characteristic of PA more accurately [37]. However, PAs does not have constant gains, their gains change with the input power (figure 2-1), so choosing the gain value to normalize the output signal is one of the key points. There are many different suggested methods in literature about choosing the normalizing gain of PA for DPD purposes. Some of the most commonly knowns are, normalizing to the maximum gain of the amplifier [38], normalizing to the gain at the maximum targeted output power [39] and normalizing the gain in a way that average power of the output of the pre distorter does not change [40]. In this project a different method, is used for gain normalization which can be described in equation 3-1.

$$y_{norm}(t) = y_{capture}(t) \times \left(\frac{mean|x(t)|}{mean|y_{capture}(t)|}\right) \quad (3\text{-}1)$$

In this method the root mean square (RMS) values of the input and the output signals are considered and the normalization of the output signal is done with these values. This method is used because of; RMS value is more reliable if the signals have high peaks (high peak to power ratio) and these peaks can mislead the normalization value. After normalization inverse PA model has been created i.e. the kernels for inverse model K_I has been estimated (figure 3-2), as in this thesis indirect learning architecture (section 2.6.1.2) has been followed. From $x(t)$ and K_I, pre distorted signal $x_{dpd}(t)$ has been generated and used as input signal to DUT and investigate the ACPR. If the ACPR do not satisfy the requirement the whole loop starts again to create the next pre distorted block to achieve the desired results. We used MATLAB environment to evaluate all the steps.

However, during the whole process, it has been figured out that, the experimental setup has two main flaws. First of them is that the VSA has the maximum capturing analysis bandwidth of 85MHz. But, to have the best performance model the PA for modeling and DPD purposes, captured output response should contain the 3rd and 5th order intermodulation products of the input signal. Therefore, with higher capturing bandwidth, the model and linearization performance can be increased. Another drawback is the measurement uncertainty from the VSA, i.e. it creates additional random noises. This problem deteriorates the modeling performance. However, this random noise wasn't observed for each test, a pattern or the reason couldn't be found. More comments on these examined in discussion part.

3.3 Results

This section discusses all the results obtain for PA behavioral modeling and the linearization results using DPD. In the thesis, three different PA from three different vendors has been used for measurement. All three PA's are designed for third (3G) and fourth (4G) generation mobile telecommunication system. Optimal supply voltages according to the vendors' recommendations are supplied to activate the PA's from a stable power supply before enabling the input stimuli signal.

3.3.1 Modeling Result

All three PA's are driven in the same compression region so that, the nonlinearities can be observed and the model performance for different methods can be compared. For all three PA's, the parameters i.e. memory order, power order, cross term orders etc. are swept for all five modeling method. Table 3-1 shows the parameters sweeping range. For example, for GMP model nonlinearity order K_a has been swept from 1 to 6 values. The sweeping is terminated when the NMSE result started to converge

to its limit. Each method's NMSE value converges to its limit after a certain level of coefficients which can be seen on each PAs corresponding NMSE vs Number of coefficients graphs.

Model	Parameter														
	Ka	Kb	Kc	Kd	Ke	Ma	Mb	Mc	Md	Me	Mf	Lb	Lc	Ld	Le
MP	1-6					1-5									
GMP	1-6	1-6	1-6			1-5	1-3	1-3				1-3	1-3		
SV	2,4,6	2,4,6	2,4,6	3	3	1-5	2-3	2-3	2-3	2-3	2-3	2-3	2-3	3	3
ACRGMP	2,4,6	4,5,6	4,5,6			1,3,5	2-4	2-4	1-3			2-4	2-4		
ACRSV	2,4,6	2,4,6	2,4,6	3-4	3-4	1,3,5	2-4	2-4	2-4	2-4	1-3	2-4	2-4	1-3	1-3

Table 3-1: PA modeling parameters sweeping range for all five models.

3.3.1.1 Modeling results for PA-1 from Vendor 1

This PA from vendor 1 has driven at 21 dBm average output power, which is at its compression region for both the test signal-1 (two 5MHz cascaded with 15MHz spacing) and test signal-2 (two 20MHz cascaded). The NMSE vs Number of coefficients graphs has been shown in figure 3-5(a) and figure 3-5(b) for test signal-1 and test signal-2 respectively. Five different curve represents five different models NMSE values with increase number of coefficients.

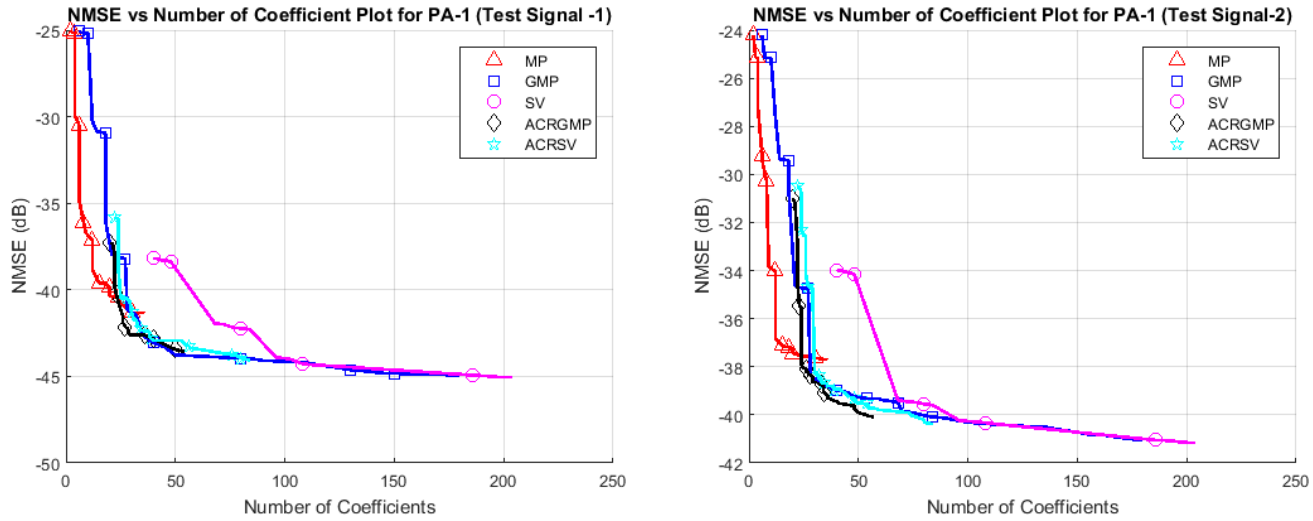

(a) *(b)*

Figure 3-5: NMSE vs Number of coefficients for PA-1 (a) Test signal-1 (b) Test signal-2

From the graph in figure 3-5 it can be seen that each method reached its limit with increase of coefficient numbers. And Table 3-2 shows the best NMSE results for each PA model considering the five methods discussed for both test signals.

PA-1 Test Signal-1																
Model	**Coefficient**	**NMSE (dB)**	**Parameter**													
			Ka	**Kb**	**Kc**	**Kd**	**Ke**	**Ma**	**Mb**	**Mc**	**Md**	**Me**	**Mf**	**Lb**	**Lc**	**Ld**	**Le**
MP	36	-41.34	6					5									
GMP	180	-44.93	6	6	6			5	3	3				3	3		
SV	204	-45.05	6	6	6	3	3	5	3	3	3	3		3	3	3	3
ACRGMP	54	-43.56	6	6	6			3	4	4	1			4	4		
ACRSV	84	-44.05	6	6	6	3	3	5	4	4	4	4	3	4	4	3	3
PA-1 Test Signal-2																	
Model	**Coefficient**	**NMSE (dB)**	**Parameter**														
			Ka	**Kb**	**Kc**	**Kd**	**Ke**	**Ma**	**Mb**	**Mc**	**Md**	**Me**	**Mf**	**Lb**	**Lc**	**Ld**	**Le**
MP	36	-37.71	6					5									
GMP	180	-41.06	6	6	6			5	3	3				3	3		
SV	204	-41.17	6	6	6	3	3	5	3	3	3	3		3	3	3	3
ACRGMP	57	-40.07	6	6	6			5	4	4	2			4	4		
ACRSV	84	-40.38	6	6	6	3	3	5	4	4	4	4	3	4	4	3	3

Table 3-2: Best NMSE result and corresponding parameter value for PA-1

For test signal-1 best lowest NMSE -45.05 dB observed for SV method and test signal-2 gives the best lowest NMSE -41.17 dB for the same method with 204 numbers of coefficients. As expected model performance for MP method is worst (NMSE value is the highest). GMP gives better result than ACRSV and ACRGMP but with almost 100 more coefficients. However, for both the test cases, ACRSV method reaches NMSE result of -44.05 dB and -40.38 dB with only 84 coefficients. So, reducing almost 59% resources the model performance reduces only within 1 dB range of best results. Therefore, considering the application of the model with limited resources for this specific PA, ACRSV method can also be considered as best method. This is a tradeoff between the model performance and number of coefficient need to be considered depending on the application of the PA model. However, one observation is that with the test signal bandwidth increases the model performance decreases. Figure 3-6 shows the modeled spectrum mimicking the measured output spectrum. This plot is for the best NMSE result shown in table 3-2. Moreover, the blue line shows the input signal spectrum, red line shows the output signal spectrum measured by experimental setup and the black dotted line is the output signal spectrum from the PA model generated from SV method.

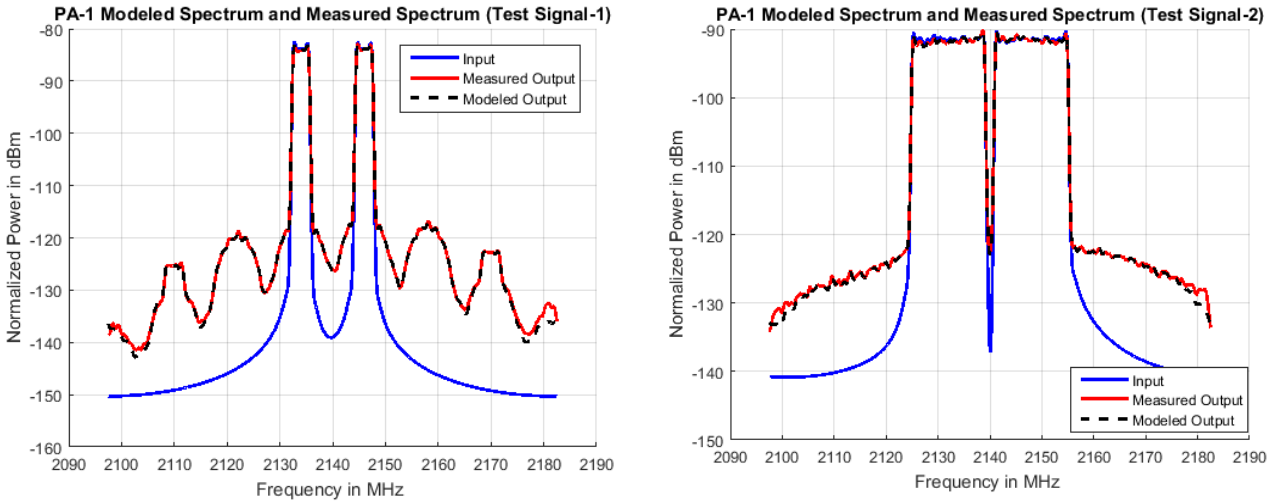

(a) *(b)*

Figure 3-6:Measured PA Output response and Modeled output response (a) Test signal-1 (b) Test signal-2

3.3.1.2 Modeling results for PA-2 from Vendor 2

This PA from vendor 2 has driven at 18.4 dBm average output power and for test signal-1 and test signal-2, which is in the compression region. The NMSE vs Number of coefficients graphs has been shown in figure 3-7(a) and figure 3-7(b) for test signal-1 and test signal-2 respectively.

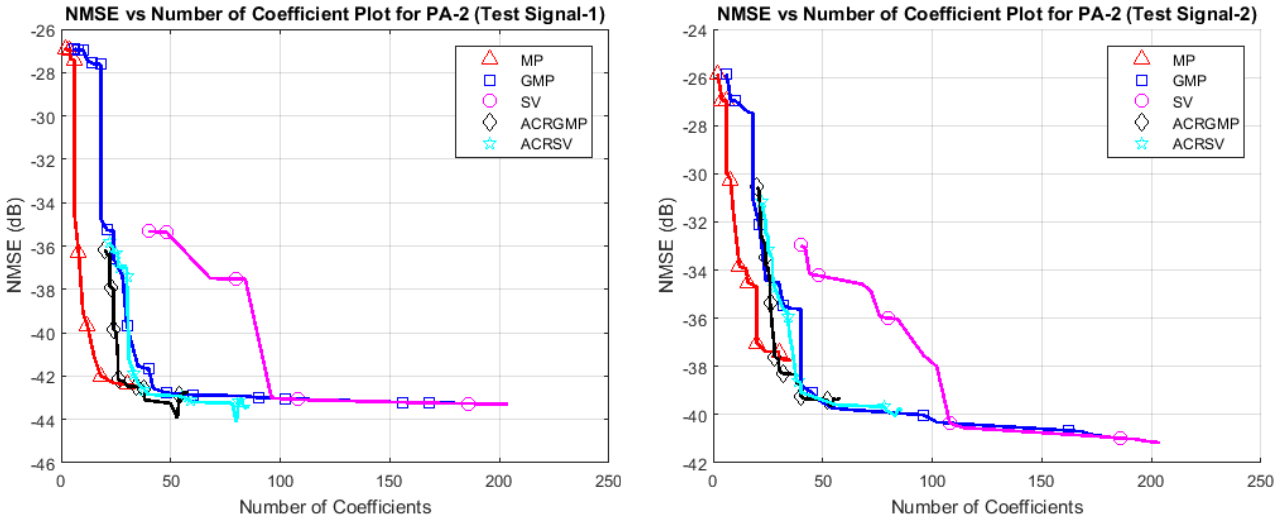

(a) *(b)*

Figure 3-7 NMSE vs Number of coefficients for PA-2 (a) Test signal-1 (b) Test signal-2

PA-2 Test Signal-1																
Model	**Coefficient**	**NMSE (dB)**	**Parameter**													
			Ka	**Kb**	**Kc**	**Kd**	**Ke**	**Ma**	**Mb**	**Mc**	**Md**	**Me**	**Mf**	**Lb**	**Lc**	**Ld**	**Le**
MP	36	-42.47	6					5									
GMP	180	-43.22	6	6	6			5	3	3				3	3		
SV	204	-43.28	6	6	6	3	3	5	3	3	3	3		3	3	3	3
ACRGMP	53	-43.95	6	6	6			1	4	4	2			4	4		
ACRSV	80	-44.13	6	6	6	4	4	1	4	4	4	4	1	4	4	3	3
PA-2 Test Signal-2																	
Model	**Coefficient**	**NMSE (dB)**	**Parameter**														
			Ka	**Kb**	**Kc**	**Kd**	**Ke**	**Ma**	**Mb**	**Mc**	**Md**	**Me**	**Mf**	**Lb**	**Lc**	**Ld**	**Le**
MP	36	-37.75	6					5									
GMP	180	-40.91	6	6	6			5	3	3				3	3		
SV	204	-41.16	6	6	6	3	3	5	3	3	3	3		3	3	3	3
ACRGMP	54	-39.67	6	6	6			3	4	4	1			4	4		
ACRSV	83	-40,15	6	6	6	4	4	3	4	4	4	4	2	4	4	3	3

Table 3-3: Best NMSE and corresponding parameter value for PA-2

From the graph in figure 3-7 we can observe the NMSE curve for PA-2 also reaches its limit with the increase coefficient number for all five methods. The best results are tabulated in Table 3-3. The best method for test signal-1 is ACRSV with -44.13 dB NMSE. Corresponding, best model performance for test signal-2 is SV with -41.16 dB. But, here ACRSV also reaches -40.15 dB with only 83 coefficients.

3.3.1.3 Modeling results for PA-3 from Vendor 3

This PA-3 from vendor 3 also driven at 17 dBm average output power and for test signal-1 and test signal-2, which is in the compression region. The NMSE vs Number of coefficients graphs has been shown in figure 3-8(a) and figure 3-8(b) for test signal-1 and test signal-2 respectively. Accordingly, table 3-4 shows the best result for each model for both the test signal.

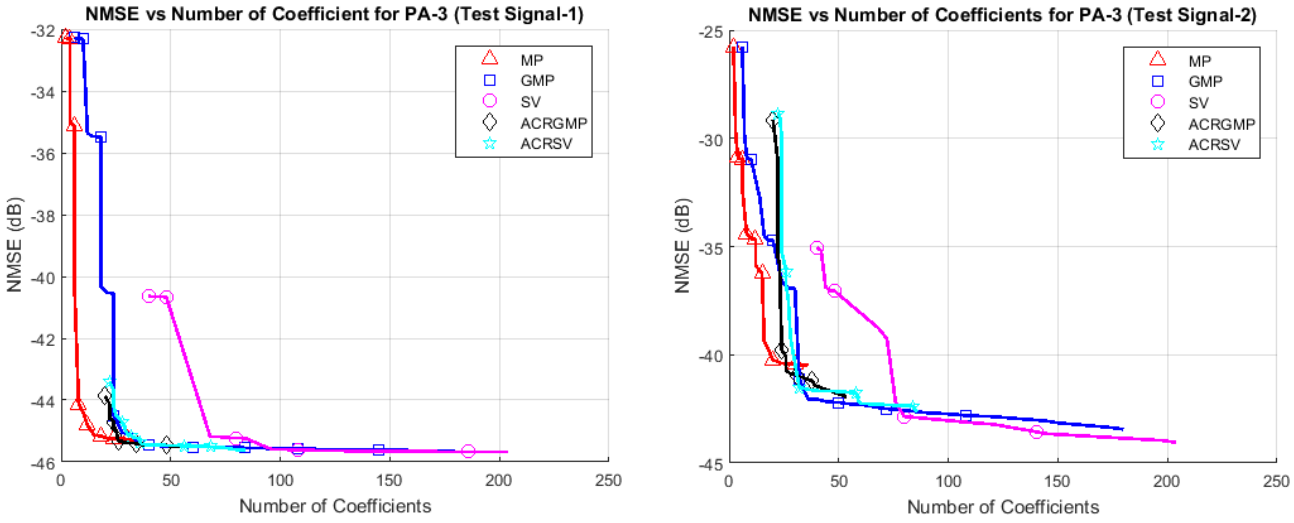

(a) *(b)*

Figure 3-8: NMSE vs Number of coefficients for PA-3 (a) Test signal-1 (b) Test signal-2

PA-3 Test Signal-1																	
Model	**Coefficient**	**NMSE (dB)**	**Parameter**														
			Ka	**Kb**	**Kc**	**Kd**	**Ke**	**Ma**	**Mb**	**Mc**	**Md**	**Me**	**Mf**	**Lb**	**Lc**	**Ld**	**Le**
MP	36	-45,28	6					5									
GMP	180	-45,64	6	6	6			5	3	3				3	3		
SV	204	-45,68	6	6	6	3	3	5	3	3	3	3		3	3	3	3
ACRGMP	54	-45,49	6	6	6			1	4	4	3			4	4		
ACRSV	84	-45,60	6	6	6	3	3	5	4	4	4	4	3	4	4	3	3
PA-3 Test Signal-2																	
Model	**Coefficient**	**NMSE (dB)**	**Parameter**														
			Ka	**Kb**	**Kc**	**Kd**	**Ke**	**Ma**	**Mb**	**Mc**	**Md**	**Me**	**Mf**	**Lb**	**Lc**	**Ld**	**Le**
MP	36	-40,49	6					5									
GMP	180	-43,45	6	6	6			5	3	3				3	3		
SV	204	-44,05	6	6	6	3	3	5	3	3	3	3		3	3	3	3
ACRGMP	54	-42,03	6	6	6			1	4	4	3			4	4		
ACRSV	84	-42,62	6	6	6	3	3	5	4	4	4	4	3	4	4	3	3

Table 3-4: Best NMSE result and corresponding parameter value for PA-3

From the graph in figure 3-8 we can observe the NMSE curve for PA-3 also reaches its lowest limit with the increase coefficient number for all five methods. The best results are tabulated in Table 3-4. The best method for test signal-1 is SV with -45.68 dB NMSE but remaining four model performance almost same as SV, only varies on decimal points. Accordingly, for test signal-2, SV method shows best model performance with -44.05 dB NMSE.

3.3.2 DPD Results

All DPD tests that are done in this thesis use the fixed parameters shown in table 3-5 for different methods. When deciding these parameters, for the common parameters between different methods the

same values has been chosen and for the non-common parameters reasonable values from the reference papers have been used. Further, PA-1 and PA-2 has been tested for DPD for test signal-1 as PA-3 could not linearize, details has been discussed in chapter 4.

Model	Parameter														
	Ka	Kb	Kc	Kd	Ke	Ma	Mb	Mc	Md	Me	Mf	Lb	Lc	Ld	Le
MP	6					5									
GMP	6	5	5			5	2	2				2	2		
SV	6	5	5	3	3	5	2	2	2	2		2	2	2	2
ACRGMP	6	6	6			5	3	3	1			3	3		
ACRSV	6	6	6	3	3	5	3	3	2	2	1	3	3	2	2

Table 3-5: Fixed Parameter for DPD Algorithm

3.3.2.1 DPD results for PA-1 from Vendor-1

The DPD algorithm is tested for the first PA-1 from Vendor-1 with an output power of 21 dBm. The output spectrum without DPD and the linearized output spectrum after implementing the pre distorter using five different methods have been shown in figure 3-9. The figure shows that ACRGMP and ACRSV method provide better performance i.e. suppression of adjacent channel power levels compare to remaining MP, GMP and SV method. Table 3-6 shows the ACLR levels. Without any DPD algorithm, the ACLR levels of the output signal is -36.7 dB and -34.23 dB which are higher than the specifications of 3GPP for LTE, which is -45 dB.

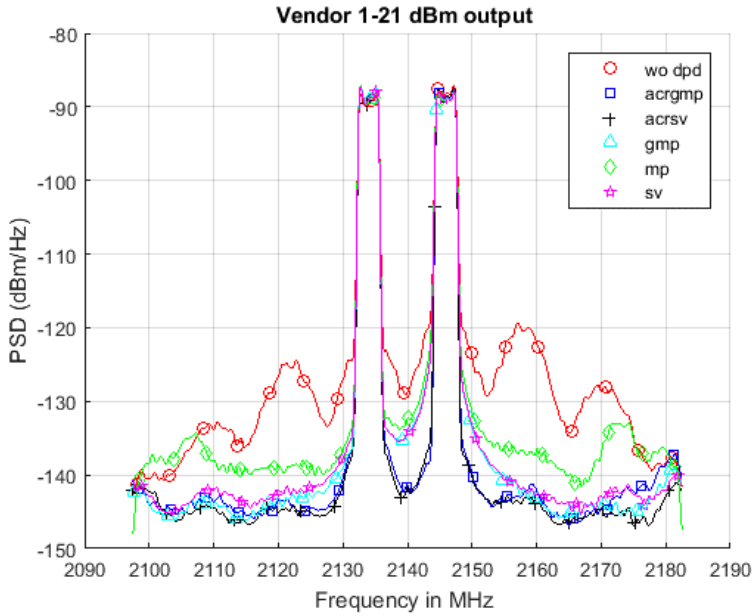

Figure 3-9: Frequency spectrum before linearization and after linearization using DPD for PA-1

Model	Lower ACLR1 (dB)	Higher ACLR1 (dB)	Coefficient Number
Without DPD	-36.7	-34.2	
MP	-46.1	-40.3	36
GMP	-48.9	-42.3	72
SV	-47.3	-42.2	108
ACRGMP	-49.5	-49.1	42
ACRSV	-50.4	-50	52

Table 3-6: ACLR results for PA-1

The ACLR values of Table 3-6 shows that MP, GMP and SV method fulfills the criteria of LTE standard -45 dB in the lower ACLR1, but for higher ACLR1 it cannot satisfy. However, ACRGMP and ACRSV satisfy both lower and higher ACLR1 levels. The best linearization performance obtains by ACRSV method and the ACLR1 reaches to -50 dB which is 5 dB lower than the requirement. Further, it suppresses 13.7 dB on lower ACLR1 side and 15.8 dB on higher ACLR1 side. ACRGMP model also shows good linearization performance with lowest coefficient numbers. Moreover, the AM/AM and AM/PM curves before and after implementing DPD are plotted in figure 3-10.

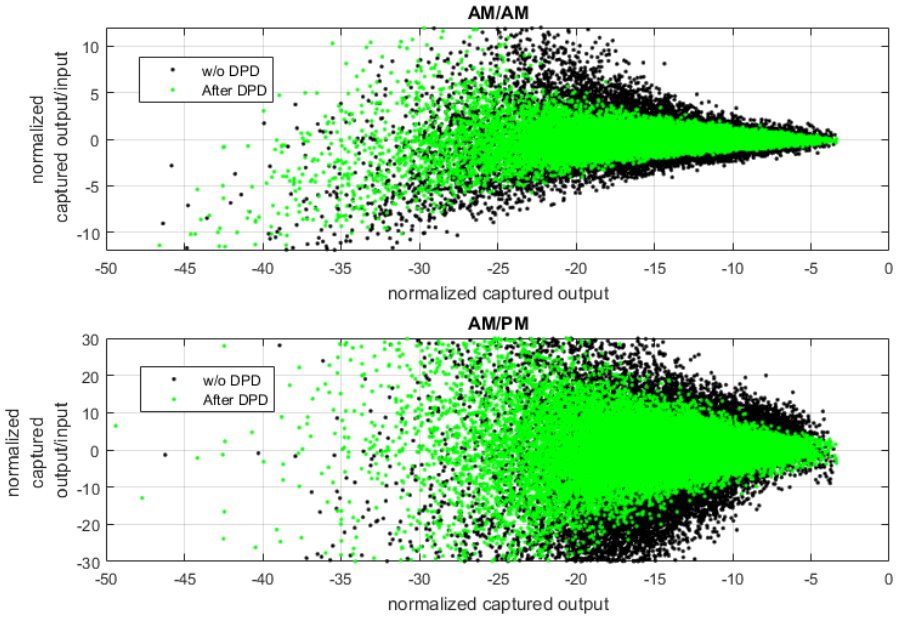

Figure 3-10: AM/AM and AM/PM curves for PA-1

The high spread at the low output power levels caused by the memory effects and the noise effect of the measurement setup which discussed at section 3.2. However, after implementation of DPD algorithm it reduces the memory spread and more over the distortion, which observed at higher power levels also compensated.

3.3.2.2 DPD Results for PA-2 from Vendor-2

Similarly PA-2 from Vendor-2 has been tested using DPD technique to linearize its performance and the PA average output power set to 18.4 dBm to operate the same at its gain compression region. The result for the output spectrum of PA has been shown in figure 3-11 and the ACLR values are shown in table 3-7.

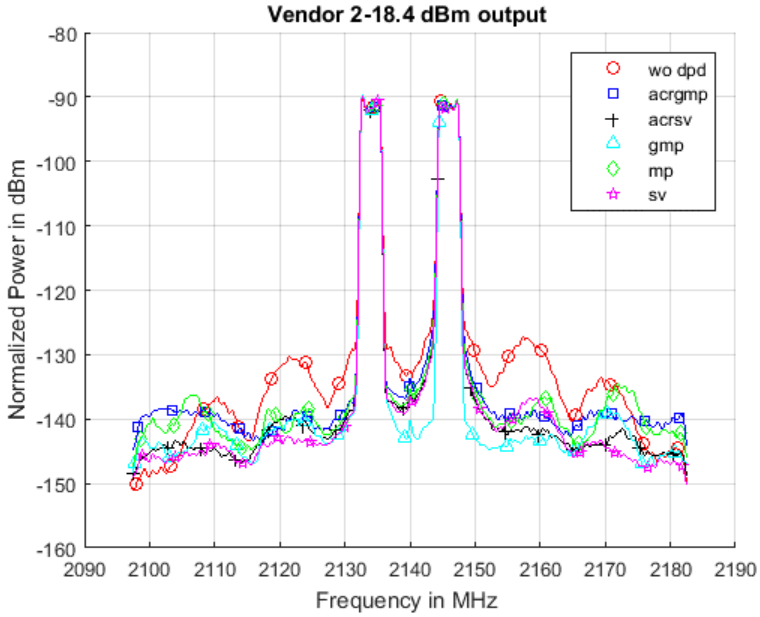

Figure 3-11: Frequency spectrum before linearization and after linearization using DPD for PA-2

Model	Lower ACLR1 (dB)	Higher ACLR1 (dB)	Coefficient Number
Without DPD	-39.4	-36.9	
MP	-46.2	-42.1	36
GMP	-48.5	-50	72
SV	-48.0	-43.1	108
ACRGMP	-46.1	-41.0	42
ACRSV	-47.4	-43.3	52

Table 3-7: ACLR results for PA-1

The ACLR values of Table 3-7 show that all five methods fulfill the standard requirement of -45 dB in the lower ACLR1. But for higher ACLR1 only GMP outperformed all other models and reaches to -50 dB. Remaining four models cannot even fulfill the requirement of -45 dB. Therefore, for PA-2 GMP method gives the best linearization performance. Details analysis of these results has been discussed in

chapter 4. The AM/AM and AM/PM curves before and after implementing DPD are plotted in figure 3-12.

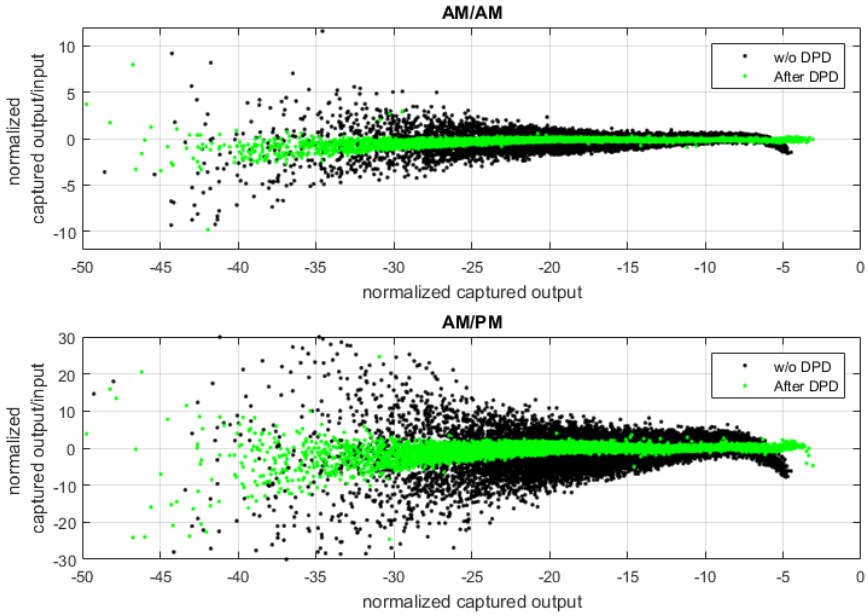

Figure 3-12: AM/AM and AM/PM curves for PA-2

Here, DPD algorithm linearizes the peak points which are at the compression region of the PA for both amplitude and phase. Along with it DPD also get rid of the memory effect i.e. the spread of the curve.

4 Discussion

To operate PA in a more efficiently it should run in the nonlinear region. And, this problem can definitely solve by using the DPD. Hence, the behavioral modeling of PA is also important. This thesis work examined five different methods of PA modeling namely MP, GMP, SV, ACRGMP and ACRSV. Later all these methods are used to create the model of PA and use it for DPD. However, this chapter will review the outcome of this thesis work by analyzing all the results describes in previous sections.

For the forward modeling results SV method gives the best modeling performance for PA-1 and PA-3 but for PA-2 ACRSV method outperform the SV method by 0.85 dB. And the modeling results for the MP method is the worst compare to other methods as expected, MP method uses only the aligned terms of the input signal and its complex envelop. But with SV, it not only added the cross terms but also added the conjugate terms. Implementation of augmented complexity reduced method (ACRGMP and ACRSV) reduces the coefficient number significantly (almost 59% for SV and 70% for GMP) compare to original method (GMP and SV) but these ACR methods gives better performance in one case (for PA-2). Further, for other two PA's model NMSE result for ACRGMP and ACRSV is within 1 dB range. So, considering available resources and application of PA model ACR methods can also be the best solution which is the tradeoff of model performance to resource usage. Special characteristic noticed for PA-3 is that, all five models give almost the same modeling results.

Moreover, for overall PAs modeling results, input test signal-2 (40MHz bandwidth signal) is worse compare to input test signal-1(20MHz bandwidth signal). It is obvious because, our measurement setup has a capturing bandwidth of 85MHz. Therefore, it cannot capture the 3^{rd} and 5^{th} intermodulation product for test signal-2 which is necessary to generate better modeling results. So, to analyze and model the effect of high bandwidth input signal to PA higher measurement capturing bandwidth is required. Accordingly, as mentioned in section 3.3.2 only test signal-1 is used for examining the linearization performance of PA using DPD, as for higher bandwidth test signal-2 it was not possible to linearize the PA performance using this measurement setup.

For linearization performance, PA-1 gives the best ACLR results for ACRSV method and for PA-2 GMP gives the best ACLR results. For PA-1 along with ACRSV method, ACRGMP also satisfy the required ACLR level compare to other three methods. Reason behind the supremacy of these two ACR methods can be explained from their mathematical equations as discussed in chapter 2. As a matter of fact these methods added nonlinear memory block along with regular cross terms and conjugate terms. Therefore, for this specific PA, ACRSV method should be used for linearization purposes. On the contrary, for PA-2 GMP method outrun all remaining four methods. These results show that, for this specific PA, the additional conjugate terms of the signal and it's envelop (i.e. SV method) decreases the inverse modeling result of PA. But, GMP's better performance than MP shows

that only addition of cross leading and lagging terms increases the inverse modelling performance. Furthermore, ACR method with the NME block also decreases the inverse modeling result and corresponding DPD results. Therefore, for this specific PA-2 NME block decreases the DPD results but the same methodology increases the DPD results for PA-1. The block that gave advantage for PA-1, can create a disadvantage for PA-2, due to their different characteristics.

Another aspects of this thesis work is, even though DPD algorithm uses the inverse behavioral PA modeling it doesn't ensure that, best forward behavioral model will give the best inverse behavioral PA model i.e. corresponding best DPD results. For both PA-1 and PA-2 best forward behavioral model did not give the required DPD results.

Finally, for the specific PAs which were characterized in this thesis work, did not give any specific best method among the five. But, these PA's models were generated, which represent their actual behavior accurately and the performance of the same also linearized using DPD technique to fulfill the standard requirement.

5 Conclusion

Due to the growing number of mobile users and the trend towards multi-band and multi-mode communication systems, high efficiency and high linearity power amplifiers are more and more desirable. Therefore, a high efficiency power amplifier with an integrated linearization technique is increasingly popular today. During this thesis work, we have analysed and implemented indirect learning Pre Distortion techniques for three different Pas along with their corresponding behavioral modeling performance. Further this thesis work provides relevant facts about the RF PA measurement technique considering the analysis bandwidth. Due to the nonlinear behavior of the device, the bandwidth of the measured output signal must be the nonlinear order times the bandwidth of the input Signal. With increasing signal bandwidths in the modern communication systems makes the measurement situation even more complicated. This can be a point of further research to use a measurement setup with a higher analysis bandwidth than the used one in this thesis. Accordingly, linearization can be analysed for higher bandwidth input signal. Moreover, this thesis work, used a fixed number of parameter for DPD implementation rather than sweeping of the parameter, though it has been done in behavioral modeling part. Further research can investigate the linearization performance of the PA's by sweeping the parameters in DPD test. Again, another sector of modeling and DPD algorithm is to estimate the best suitable parameter. These might examine also in future research.

References

1. 3GPP technical specification, TS 36, February 2016 [online] Available: http://www.3gpp.org/ftp/Specs/archive/36 series/
2. A. Zhu, P. J. Draxler, J. J. Yan, T. J. Brazil, D. F. Kimball, and P. M. Asbeck, "Open-Loop Digital Predistorter for RF Power Amplifiers Using Dynamic Deviation Reduction-Based Volterra Series," in *IEEE Transactions on Microwave Theory and Techniques*, vol. 56, no. 7, pp. 1524-1534, July 2008.
3. S. C. Cripps, *Advanced Techniques in RF Power Amplifier Design*. Boston, MA: Artech House, 2002.
4. J. H. K. Vuolevi and T. Rahkonen, *Distortion in RF Power Amplifiers*. Boston, MA: Artech House, 2003.
5. P. B. Kennington, *High Linearity RF Amplifier Design*. Norwood, MA: Artech House, 2000.
6. R. W. Erickson and D. Maksimovic, *Fundamentals of Power Electronics*, 2nd ed. Norwell, MA: Kliwer, 2000.
7. H. Krauss, C. Bostian, and F. Raab, *Solid State Radio Engineering*, New York: Wiley, 1980, pp. 432-467.
8. D. Pozar, *Microwave Engineering,* 3rd ed. New York: Wiley, 2013.
9. A. Abdalla, O Hammi, A. Kwan, A. Zerguine, and F. Ghannouchi, "A Novel Weighted Memory Polynomial For Behavioral Modeling And Digital Predistortion Of Nonlinear Wireless Transmitters" in *IEEE Transactions on Industrial Electronics*, vol. 63, no. 3, pp. 1745-1753, Mar. 2016.
10. P. Roblin, D. Root, J. Verspecht, Y. Ko, and J. Teyssier, "New Trends for The Nonlinear Measurement And Modeling Of High-Power RF Transistors And Amplifiers With Memory Effects", in *IEEE Transactions on Microwave Theory and Techniques*, vol. 60, no. 6, pp. 1964-1978, June 2012.
11. A. A. Moulthrop, C. J. Clark, C. P. Silva, and M. S. Muha, "A dynamic AM/AM and AM/PM measurement technique", in *IEEE Microwave Symposium Digest,* vol. 3, pp. 1455-1458, Aug. 2002.
12. J. C. Pedro and S. A. Maas, "A comparative overview of microwave and wireless power-amplifier behavioral modeling approaches," in *IEEE Transactions on Microwave Theory and Techniques,* vol. 53, no. 4, pp. 1150–1163, April 2005.
13. C. J. Clark, C. P. Silva, A. A. Moulthrop, and M. S. Muha, "Power-amplifier characterization using a two-tone measurement technique," in *IEEE Transactions on Microwave Theory and Techniques*, vol. 50, no. 6, pp. 1590–1602, June 2002.

14. H. Ku, “Behavioral Modeling of Nonlinear RF Power Amplifiers for Digital Wireless Communication Systems with Implications for Predistortion Linearization Systems,” Ph.D. dissertation, Dept. of Elect. Eng., Georgia Institute of Technology, 2003.
15. J. Verspecht, and D. E. Root., “Polyharmonic Distortion Modeling,” in *IEEE Microwave Magazine,* vol.7, pp.44-57, June 2006.
16. M. Isaksson, D. Wisell and D. Ronnow, "A comparative analysis for behavioral models of rF power amplifiers", in *IEEE Transactions on Microwave Theory and Techniques*, vol. 54, no. 1, pp. 348-359, Jan. 2006.
17. V. Volterra, *Theory of Functionals and of Integrals and Integro-Differential Equations,* Madrid 1927 (Spanish), translated version reprinted New York: Dover Publications, 1959.
18. J. S. Bendat, *Nonlinear System Techniques and Applications*. New York: Wiley, 1998.
19. H. Ku, and J. S. Kenney, “Behavioral modeling of nonlinear RF power amplifiers considering memory effects,” in *IEEE Transactions on Microwave Theory and Techniques*, vol. 51, no. 12, pp. 2495–2504, Dec. 2003.
20. D. R. Morgan, Z. Ma, J. Kim, M. G. Zierdt, and J. Pastalan, “A generalized memory polynomial model for digital predistortion of RF power amplifiers,” in *IEEE Transactions on Signal Processing*, vol. 54, no. 10, pp. 3852–3860, Oct. 2006.
21. Y. J. Liu, J. Zhou, W. Chen and B. H. Zhou, "A robust augmented complexity-reduced generalized memory polynomial for wideband RF power amplifiers", in *IEEE Transactions on Industrial Electronics*, vol. 61, pp. 2389-2401, May 2014.
22. T. Du, C. Yu, J. Gao, Y. Liu, S. Li, and Y. Wu, "A new accurate volterra-based model for behavioral modeling and digital predistortion of RF power amplifiers," *Progress In Electromagnetics Research C*, Vol. 29, 205-218, 2012.
23. Du, T., C. Yu, Y. Liu, J. Gao, S. Li, and Y. Wu, “A new accurate Volterra-based model for behavioral modeling and digital predistortion of RF power amplifiers,” *Progress In Electromagnetics Research C*, Vol. 29, 205–218, 2012.
24. S. M. Kay, *Fundamentals of Statistical Processing*, Volume I: Estimation Theory, Prentice Hall Signal Processing Series. Prentice Hall Professional Technical Reference, 1993.
25. S. Haykin, *Adaptive Filter Theory*. Prentice Hall, Englewood Cliffs, New Jersey, 2013.
26. T. Gotthans, G. Baudoin and A. Mbaye, "Optimal order estimation for modeling and predistortion of power amplifiers", in *Microwaves, Communications, Antennas and Electronics Systems (COMCAS)*, 2013 IEEE International Conference on, Tel Aviv, 2013.
27. B. O'Brien, J. Dooley, A. Zhu and T. J. Brazil, "Estimation of Memory Length for RF Power Amplifier Behavioral Models," in *2006 European Microwave Conference*, Manchester, 2006.

28. X. He and H. Asada, "A New Method for Identifying Orders of Input-Output Models for Non-linear Dynamic Systems," in *American Control Conference, 1993*, San Francisco, CA, USA, 1993.
29. K. Y. Chan and A. Bateman, "Analytical and Measured Performance of the Combined Analog Locked Loop Universal Modulator (Callum)," in *IEEE Proceedings-Communications*, vol. 142, issue 5, pp. 297-306, Oct, 1995.
30. P. B. Kenington, *High-linearity RF Amplifier Design*., 685, Canton Street, Norwood, MA Artech House, 2000.
31. M. Schetzen, *The Volterra and Wiener Theories of Nonlinear Systems*, New York: Wiley, 1980
32. J. Tsimbinos, "Identification and compensation of nonlinear distortion," Ph.D. dissertation, Dept. of Elect. Eng., University of South Australia, 1995.
33. M. Schetzen, "Theory of pth-order inverses of nonlinear systems, Circuits and Systems," in *IEEE Transactions* on, vol. 23, no. 5, pp. 285– 291, may 1976
34. C. Eun, and E.J. Powers, "A new volterra predistorter based on the indirect learning architecture," in *Signal Processing, IEEE Transactions*, vol. 45, no. 1, pp. 223 –227, Jan 1997.
35. J. Chani-Cahuana, C. Fager and T. Eriksson, "A new variant of the indirect learning architecture for the linearization of power amplifiers," in *Microwave Conference (EuMC), 2015 European*, Paris, 2015, pp. 1295-1298.
36. The European table of frequency allocations and applications in the frequency range 8.3 KHz to 3000 GHz (ECA table), February 2016 [online] http://www.erodocdb.dk/docs/doc98/official/pdf/ERCRep025.pdf
37. L. Aladrén, P. García-Dúcar, P. L. Carro and J. de Mingo, "Digital predistortion optimization using normalization gain adjustment in wideband systems," in *Microwave Conference (EuMC), 2013 European,* Nuremberg, 2013, pp. 420-423.
38. K. J. Muhonen, M. Kavehrad, and R. Krishnamoorthy, "Look-up table techniques for adaptive digital predistortion: a development and comparison," in *IEEE Transactions on Vehicular Technology*, vol. 49, no. 5, pp. 1995–2002, Sep 2000.
39. A. Zhu, P. J. Draxler, J. J. Yan, T. Brazil, D. F. Kimball, and P. M. Asbeck, "Open-loop digital predistorter for RF power amplifiers using dynamic deviation reduction-based volterra series," in *IEEE Transactions on Microwave Theory and Techniques*, vol. 56, no. 7, pp. 1524–1534, July 2008.
40. O. Hammi, and F. M. Ghannouchi, "Power alignment of digital predistorters for power amplifiers linearity optimization," in *IEEE Transactions on Broadcasting,* vol. 55, no. 1, pp. 109–114, March 2009.